

## Multi-wavelength investigation of a massive toroidal candidate G24.78+0.08-A2

S. Vig<sup>1,2\*</sup>, R. Cesaroni<sup>2</sup>, L. Testi<sup>2,3</sup>, M.T. Beltrán<sup>2,4</sup>  
and C. Codella<sup>5</sup>

<sup>1</sup>*Department of Physics, Indian Institute of Technology Madras, Chennai 600036, India*

<sup>2</sup>*INAF-Osservatorio Astrofisico de Arcetri, Largo E. Fermi 5, I-50125 Firenze, Italy*

<sup>3</sup>*ESO, Karl Schwarzschild str. 2, D-85748 Garching, Germany*

<sup>4</sup>*Departament d'Astronomia i Meteorologia, Universitat de Barcelona, Spain*

<sup>5</sup>*INAF-Istituto di Radioastronomia, Sezione di Firenze, Largo E. Fermi 5, I-50125 Firenze, Italy*

**Abstract.** G24.78+0.08 is a massive star-forming region where three large massive rotating structures (toroids), have been found around massive (proto)stars. We have carried out a detailed infrared and radio investigation of one of the toroidal candidates, G24-A2, using observations from VISIR-VLT and VLA and we speculate the scenario of the environment in the vicinity of the central exciting object(s). Compact mid-infrared emission is observed only from one source in the G24.78+0.08 region and this is likely to be associated with G24-A2. The radio spectral index ( $\sim 1$ ) points towards the possibility of this emission being from an ionised jet or an HII region with a density gradient. The  $\text{NH}_3(2, 2)$  emission from the main component is optically thick and appears self-absorbed at blue-shifted velocities. The velocity distributions of the  $\text{NH}_3$  lines can be explained by a motion which is a combination of rotation and expansion.

### 1. Introduction

We investigate the nature of the environment in the vicinity of G24.78+0.08 (hereafter G24) where large massive rotating structures (called toroids) have been found around massive (proto)stars (Beltrán et al. 2004). G24 is a high mass star-forming region located at a distance of 7.7 kpc. It comprises a group

---

\*e-mail: sarita@iitm.ac.in

of young high-mass (proto)stars in different evolutionary phases embedded in their parental cores. One of the cores is G24-A from which large scale  $^{12}\text{CO}$  bipolar outflow has been observed (Furuya et al. 2002). This core has been resolved into G24-A1 and G24-A2 based on high resolution line and continuum mapping (Beltrán et al. 2004). Here, we probe the nature of G24-A2 using multi-wavelength studies from VLT-VISIR and VLA (Vig et al. 2008).

## 2. Observations

Mid-infrared observations of G24 using VISIR have been carried out. VISIR is the ESO-VLT imager and spectrograph for the mid-infrared band mounted on the Cassegrain focus of the VLT Unit Telescope 3 (Melipal). The imaging through the PAH2.2 (11.88  $\mu\text{m}$ ) and Q2 (18.72  $\mu\text{m}$ ) filters was carried out on the night of 13 July 2005. The airmass at the time of observations was 1.1–1.3, and the optical seeing was better than 1". The VISIR data reduction pipeline provided by ESO was used to reduce the data.

The radio observations were made on 21 April 2005 with 26 antennas of the NRAO Very Large Array (VLA) in the B-configuration. We measured the (2,2) inversion transition of ammonia and the 1.3 cm continuum emission. Bandpass and phase were calibrated by observing 1832–105 and the flux density scales were derived by observing 3C286. Line cubes were restored with a clean beam of 0."4 or 0."8 obtaining a final rms noise of 0.4 mJy/beam. The synthesized beam and rms of the continuum image are 0."30  $\times$  0."24 and 0.15 mJy/beam respectively.

## 3. Results

The VISIR images of G24-A at 11.9 and 18.7  $\mu\text{m}$  show emission from a single source, likely to be associated with G24-A2. The source is unresolved at both wavelength bands. The dereddened fluxes ( $A_V = 14$  mag corresponding to 1.8 mag per kpc) are 130 and 120 mJy at 11.9 and 18.7  $\mu\text{m}$ , respectively.

The radio continuum emission from G24-A2 at 1.3 cm is shown as contours in Fig. 1 (left). The radio flux is  $0.86 \pm 0.07$  mJy. The interferometric observations of the  $\text{NH}_3(2,2)$  inversion transition with 0."4 angular resolution allow us to probe the molecular gas around the subcore A2. The correlator-setup of the VLA allows us to probe the main line as well as the two inner satellites of  $\text{NH}_3(2,2)$ , shown in Fig. 1 (middle). From the spectrum, we observe that the ‘main’ component is asymmetrical suggesting either self-absorption or presence of other components along the line-of-sight and most of the emission is at velocities greater than the systemic velocity of the source,  $V_{\text{LSR}} \sim 111$  km  $\text{s}^{-1}$ . From the ratio of line intensities, we obtain an optical depth of  $< 18$  and a total

column density  $N(\text{NH}_3) < 1.2 \times 10^{18} \text{ cm}^{-2}$ . The integrated emission from the main component towards G24-A2 is shown as grayscale in Fig. 1 (left).

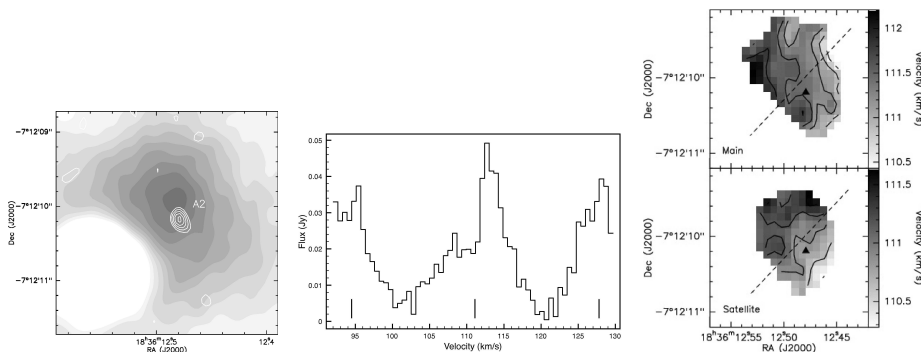


**Figure 1.** (Left)  $\text{NH}_3$  emission averaged over the main component with grayscale levels ranging from 0 (white) to 10 mJy/beam (deep gray) in steps of 1 mJy/beam where beam is  $0.''8$ . The white contours depict the 1.3 cm radio continuum emission. (Middle) Spectrum of  $\text{NH}_3(2,2)$  averaged over the emission from the entire G24-A2 region. The main component in the centre can be seen along with the two inner satellites on either side. The centres of the lines corresponding to the rest frequency of the  $\text{NH}_3$  main line and satellites are marked near the base for a  $V_{\text{LSR}} = 111 \text{ km s}^{-1}$ . (Right) The velocity distribution towards G24-A2 from the (top) main component and (bottom) satellite of  $\text{NH}_3(2,2)$  transition. The triangle marks the location of the radio continuum emission at 1.3 cm. The dashed line represents the direction parallel to the  $^{12}\text{CO}$  outflow axis. The contour levels range from 110.3 to 111.8  $\text{km s}^{-1}$  in steps of  $0.3 \text{ km s}^{-1}$ .

#### 4. Nature of G24-A2

The radio continuum emission associated with G24-A2 is unresolved as well as weak. High angular resolution maps ( $\sim 60 \text{ mas}$ ) of G24-A (Beltrán et al, 2007) at 1.3 cm and 7 millimetre does not show the presence of any emission at the location of A2 whereas point-like emission was detected with a resolution of  $0.''25$  at 1.3 cm and  $0.''48$  at 7 mm. This indicates that the radio continuum emission is from a region larger than 60 mas and the emission is too weak to be detected at such high angular resolutions. We, therefore, obtain limits on the diameter  $D$  of this source:  $1000 \text{ AU} < D < 2000 \text{ AU}$ . It is unlikely that this radio continuum emission is optically thick free-free emission as the measured brightness temperature is  $30 \text{ K} < T_B < 110 \text{ K}$ . For optically thick emission,  $T_B$  is expected to be at least  $\sim 10^3 \text{ K}$ . Recent continuum measurements at 3.6 cm with the VLA have led to the detection of G24-A2 with a flux of 0.3 mJy (Beltrán et al., personal communication). This gives a spectral index of  $\sim 1$  between 1.3 and 3.6 cm suggesting that the emission could be from a jet or an HII region with a density gradient.

Next, we attempt to understand the spectral signatures of the  $\text{NH}_3$  emission from different parts of the region associated with G24-A2. Combining the satellite lines on either side of the main component to obtain the full profile of a single satellite line, we have been able to obtain the velocity distribution traced by the satellite emission. We have obtained velocity maps as the first moment (i.e. intensity weighted velocity of the spectral line) of the main and satellite components, shown in Fig. 1 (right). It is interesting to note that the velocity distribution of the satellite line is found to be similar to that obtained using the  $\text{CH}_3\text{CN}(12-11)$  line by Beltrán et al. 2004. This can be interpreted as rotation of G24-A2 as suggested by them. On the other hand, the velocity distribution of the  $\text{NH}_3(2,2)$  main component shows a similar trend but oriented E-W rather than NE-SW like in the case of the satellite and  $\text{CH}_3\text{CN}$  lines. We believe this is due to the non-gaussian shape of the main line which shows self-absorption at blue-shifted velocities indicating an expanding envelope. In the present case, the expansion is likely to be due to the outflow detected from G24-A. Either A1 or A2 could be powering the outflow as both toroids in A1 and A2 are perpendicular to the outflow axis (see Fig. 2).

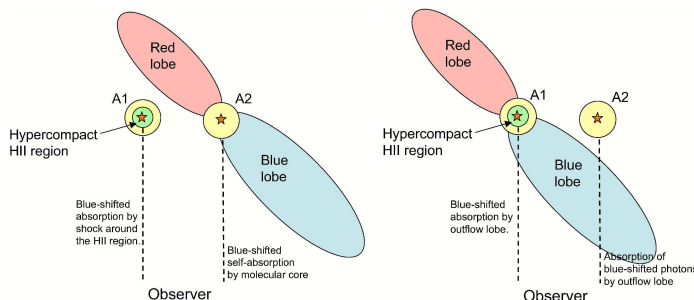


**Figure 2.** Schematic picture of G24-A showing two possible scenarios: (left) A2 is the origin of the outflow, and (right) A1 is powering the outflow. The larger circles around A1 and A2 represent the hot molecular cores, while the smaller circle around A1 represents the hypercompact HII region. Here, the dashed lines are parallel to the line-of-sight of the observer who is located at the bottom of the figure.

We consider two scenarios. In the first case, A2 is powering the outflow. The expanding gas can produce the red asymmetry seen towards the centre in the main  $\text{NH}_3$  component. The absence of such an asymmetry in the satellite line is explained because this emission is more optically thin. This expansion velocity field when combined with the one due to rotation, will explain the velocity distribution obtained for G24-A2. For the sake of completeness, we note that the broad blue-shifted wing seen in absorption of the  $\text{NH}_3(2,2)$  line towards G24-A1 (Beltrán et al. 2006) is due to the compressed layer of gas in the post-shock at the border of the hypercompact HII region imaged by Beltrán et al. (2007). In the second scenario, we assume that A1 is the driver of the outflow. In such a situation, the blue lobe of the outflow would pass in front of A2. If the  $\text{NH}_3$  column density in the blue lobe is sufficiently high, the blue part

of the  $\text{NH}_3$  line emitted by A2 will be absorbed resulting in a skewed profile with the intensity of the red part larger than that corresponding to the blue. This also explains the broad blue-shifted absorption in the main  $\text{NH}_3(2,2)$  line detected towards A1 as due to absorption in the densest part of the blue lobe towards the A1 HII region. Although we have considered two simple scenarios with either A2 or A1 being the source of the outflow, we believe the former to be more plausible. This is because the larger  $\text{NH}_3(2,2)$  optical depth needed in the latter would imply very large  $\text{NH}_3$  column density in the outflow lobe. Further, the emission from the  $\text{NH}_3(2,2)$  satellite (as well as  $\text{CH}_3\text{CN}$ ) is from denser gas closer to the central object, so that it seems unlikely that the  $\text{NH}_3$  main line emission originates from a different region. Finally, we note that the proposed scenarios do not rule out the possibility that two parallel outflows (one from A1, the other from A2) exist.

## References

- Beltrán M. T., Cesaroni R., Ner R., et al., 2004, *ApJ*, 601, 187  
Beltrán M. T., Cesaroni R., Codella C., et al., 2006, *Nature*, 443, 427  
Beltrán M. T., Cesaroni R., Moscadelli L., et al., 2007, *A&A*, 471, 13  
Cesaroni R., Galli D., Lodato G., et al., 2007, *Protostars and Planets V*, 197  
Furuya R. S., Cesaroni R., Codella C., et al., 2002, *A&A*, 390, 1  
Vig S., Cesaroni R., Testi L., et al., 2008, *A&A*, 488, 605